SUPPORTING INFORMATION

Intermediate Species in the Crystallization of Sodium Aluminate Hydroxy Hydrates

Trent R. Graham,[†,*] Mateusz Dembowski,[†] Jian Zhi Hu,[†,⊥] Nicholas R. Jaegers,[†,‡,⊥] Xin Zhang,[†] Sue B. Clark,[€,§] Carolyn I. Pearce,[€] and Kevin M. Rosso[†,*]

†Physical and Computational Sciences Directorate, Pacific Northwest National Laboratory, Richland, Washington 99354, United States

⊥Institute for Integrated Catalysis, Pacific Northwest National Laboratory, Richland, Washington 99354, United States

‡The Voiland School of Chemical and Biological Engineering, Washington State University, Pullman, Washington 99164, United States

€Energy and Environment Directorate, Pacific Northwest National Laboratory, Richland, Washington 99354, United States

§Department of Chemistry, Washington State University, Pullman, Washington 99164, United States

CORRESPONDING AUTHORS

*Trent R. Graham, E-mail: trenton.graham@pnnl.gov
*Kevin M. Rosso, E-mail: Kevin.rosso@pnnl.gov

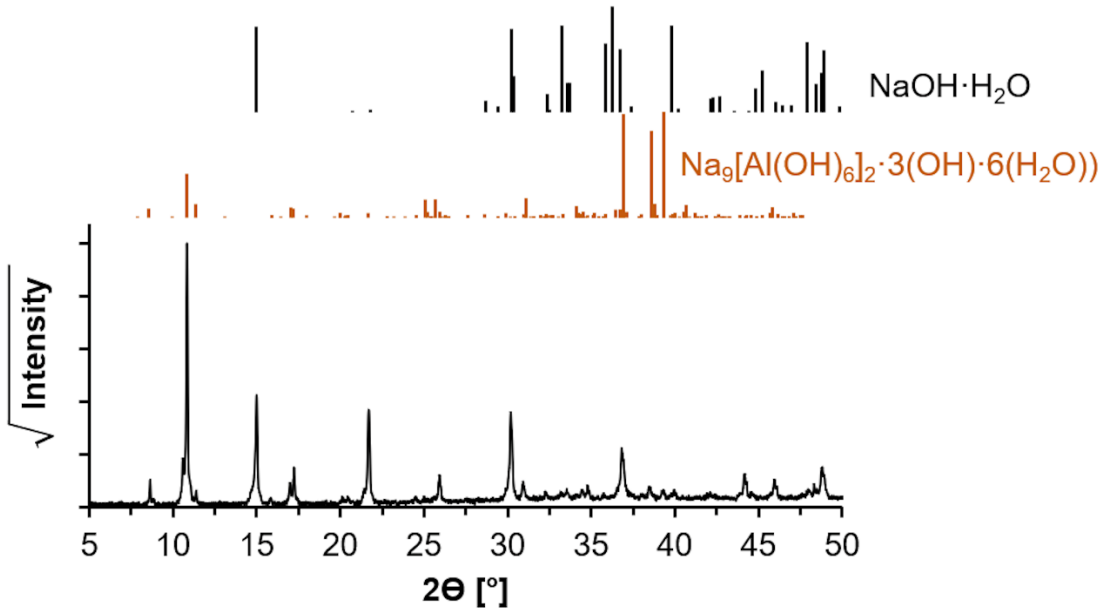

Figure S1. X-ray diffraction of nonasodium bis(hexahydroxyaluminate) trihydroxide hexahydrate ($Na_9[Al(OH)_6]_2 \cdot 3(OH) \cdot 6(H_2O)$). The sample was loaded into a sealed XRD cell equipped with Kapton windows in an N_2-filled glovebox and transported to the diffractometer for analysis. XRD pattern acquisition was performed on a Philips X'pert Multi-Purpose diffractometer (MPD, PANAlytical Almelo, The Netherlands), equipped with a fixed Cu anode operating at 40 mA and 50 kV. While significant preferential orientation is present, the obtained pattern can be approximated by a combination of NSA and $NaOH \cdot H_2O$ with a relative abundance of 3:1 (NSA:$NaOH \cdot H_2O$), determined with TOPAS (v5.). While the units of the diffractogram are displayed with units of counts$^{0.5}$, the traces are shown on a linear scale.

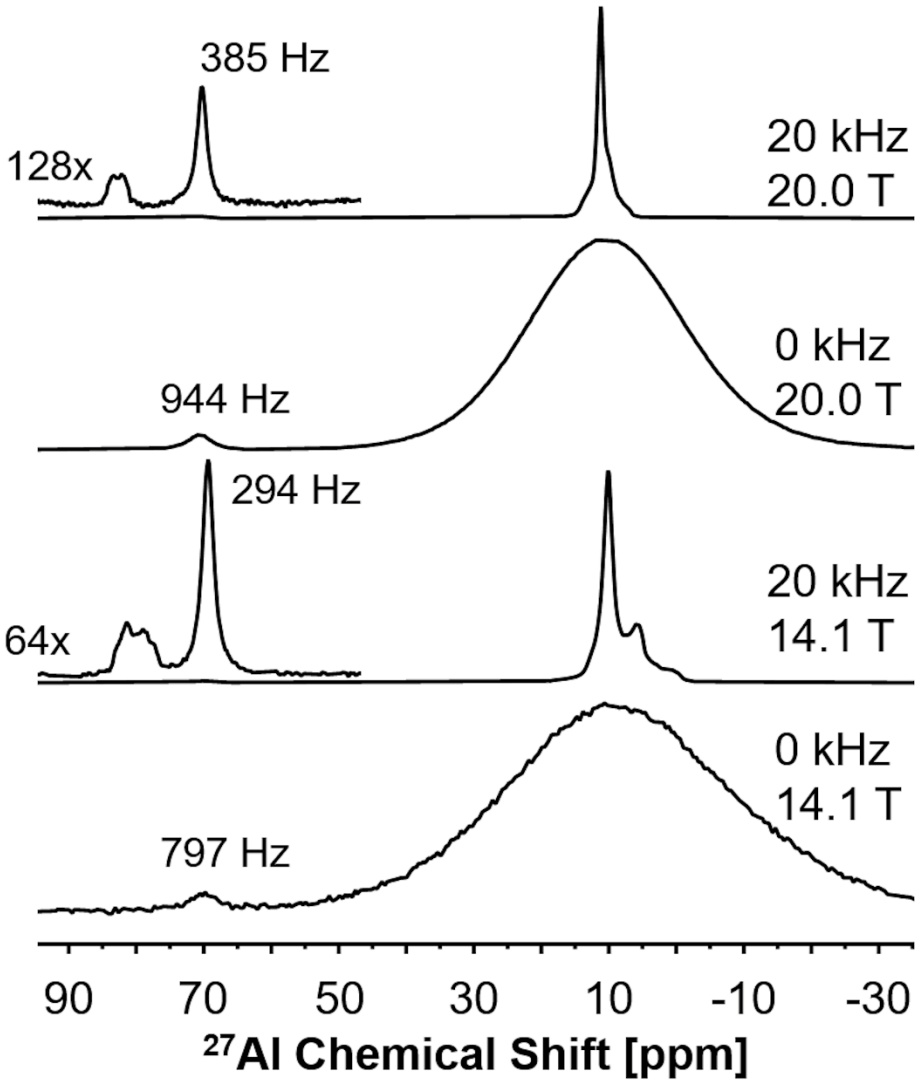

Figure S2. ^{27}Al MAS NMR spectra at a field strength of 20.0 and 14.1 T of the $Na_9[Al(OH)_6]_2 \cdot 3(OH) \cdot 6(H_2O)$ sample comparing static (w_r = 0 kHz) and acquisition with 20 kHz magic angle spinning rate (w_r). Magnifications of the tetrahedrally coordinated Al^{3+} region are vertically offset over the ^{27}Al MAS NMR spectra. While the full width at half maximum (fwhm) of the resonance assigned to the mother liquor at ca. 70 ppm decreases upon spinning, the decrease is much less than the reduction of breadth of the solid-phase octahedral resonances at 10 ppm and the tetrahedral phase resonance assigned to $Na_2Al_2O(OH)_6$ at ca. 80 ppm.

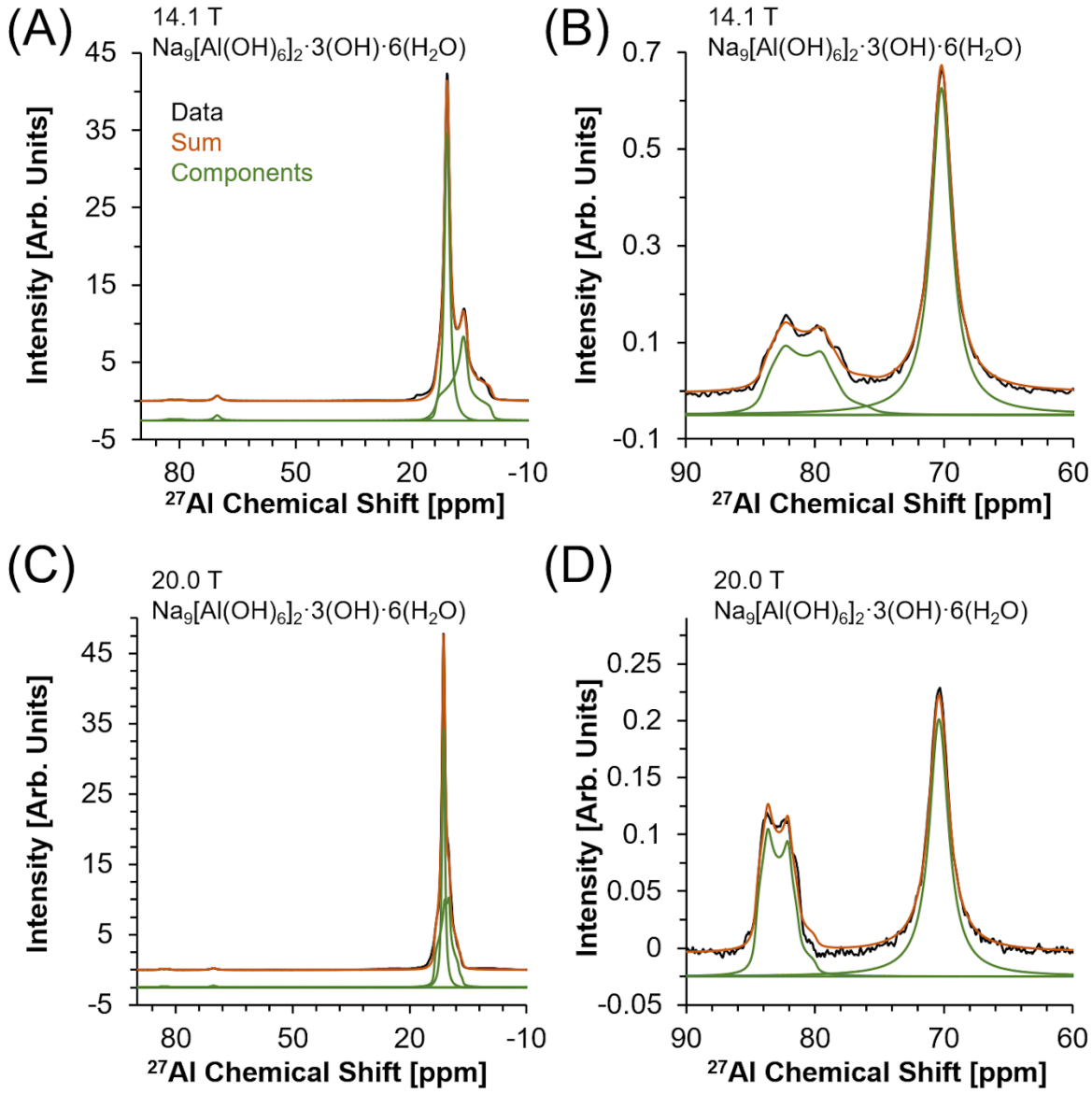

Figure S3. ^{27}Al MAS NMR spectra of nonasodium bis(hexahydroxyaluminate) trihydroxide hexahydrate (NSA, $Na_9[Al(OH)_6]_2{\cdot}3(OH){\cdot}6(H_2O)$) at (A) 14.1 T and (B) at 14.1 T with a magnified view of the tetrahedral coordinated Al^{3+} NMR region. (C) ^{27}Al MAS NMR of NSA at 20.0 T and (D) at 20.0 T with a magnified view of the tetrahedral coordinated Al^{3+} NMR region. The data is illustrated in black, the summation is in orange, and the individual line shapes are offset in green. See Table S1 for a summary of the line shape parameters.

Table S1. Quadrupolar coupling parameters for ^{27}Al MAS NMR spectra

Field Strength [T]	Sample	Line #	Isotropic Chemical Shift [ppm]	Quadrupolar Coupling Coefficient [MHz]	Asymmetry Parameter	Line Broadening [ppm]	Integral [%]
14.1	NSA	1	84.6	3.8	0.3	1.1	0.6
		2	70.2*	1.9**	n.a.	n.a.	1.3
		3	13.9	4.6	0.9	0.7	45.5
		4	11.4	1.3	0.0	1.5	52.7
20.0	NSA	1	84.9	4.0	0.3	0.4	0.4
		2	70.4*	1.8**	n.a.	n.a.	0.6
		3	13.8	4.8	0.7	0.5	54.4
		4	11.6	1.6	0.0	0.8	44.6
14.1	$K_2Al_2O(OH)_6$	1	81.9	4.5	0.3	1.3	100
20.0	$K_2Al_2O(OH)_6$	1	81.6	4.5	0.3	0.9	100

Note: Line 2 in the NSA sample at 14.1 and 20.0 T is represented by a Lorentzian line shape with a peak position (*, ppm) and full width at half max (**, ppm). Quadrupolar line shapes were calculated in DMFIT (release #20180327) and utilized the Qmas 1/2 model, which assumes infinite spinning rates. The line deconvolution and experimental spectra of the $K_2Al_2O(OH)_6$ standards are shown in the main text. The quadrupolar coupling parameters for the ^{27}Al MAS NMR spectrum of NSA crystals at 14.1 T are also detailed in a separate study.[1]

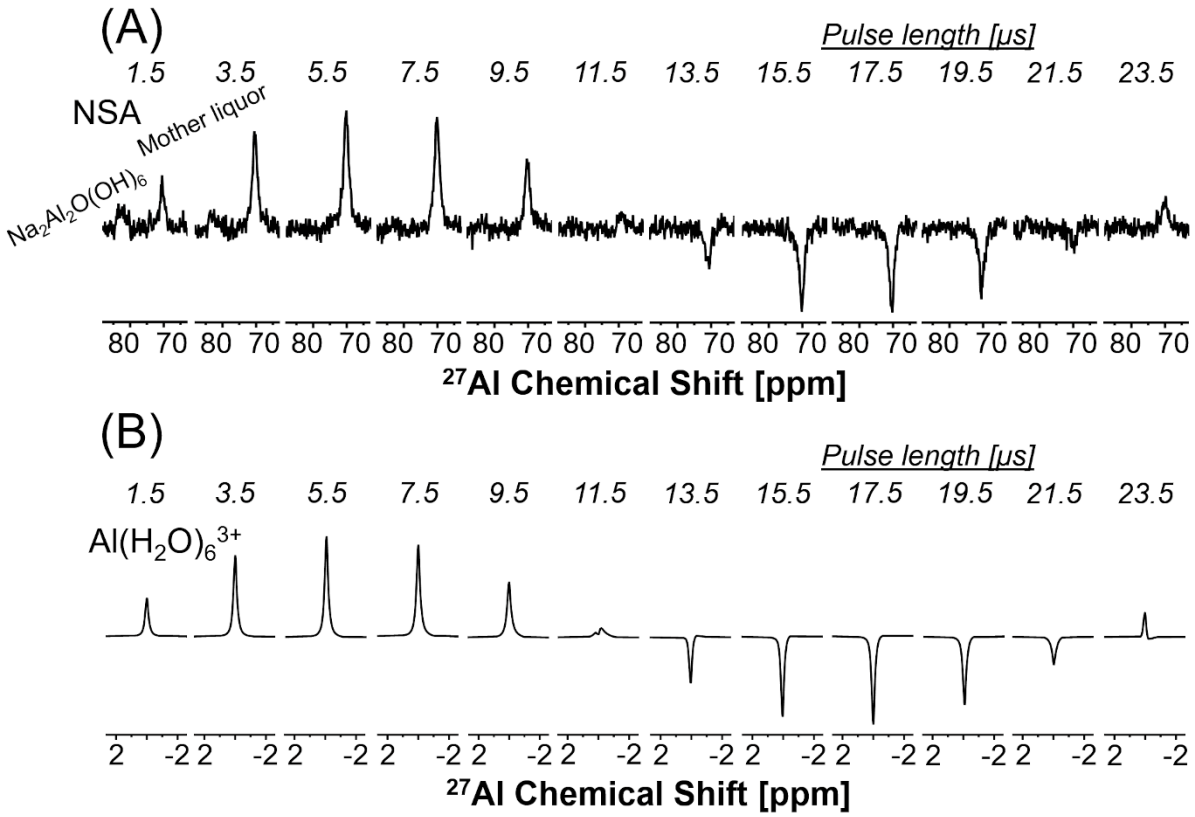

Figure S4. ^{27}Al MAS NMR pulse length nutation experiments at 20.0 T at a temperature of 20°C. (A) The tetrahedral coordinated Al^{3+} NMR spectral region of NSA crystals. (B) The $Al(H_2O)_6^{3+}$ standard prepared via dissolution of $Al(NO_3)_3 \cdot 9H_2O$ (≥98%, Sigma-Aldrich) in H_2O. Acquisition utilized a delay between experiments (d1) of 1 second. Spectra were analyzed in Mestrenova, where 20 Hz line broadening was applied. The ^{27}Al resonance assigned to the mother liquor (ca. 70 ppm) and the $Al(H_2O)_6^{3+}$ standard exhibit sinusoidal behavior, likely due to molecular tumbling in liquid-state eliminating quadrupolar coupling effects. In contrast, the dependence of the ^{27}Al resonance assigned to the $Na_2Al_2O(OH)_6$ species (ca. 80 ppm) does not exhibit sinusoidal behavior, has a signal maximum at a shorter pulse duration, and becomes vanishingly weak in intensity at long pulse durations.

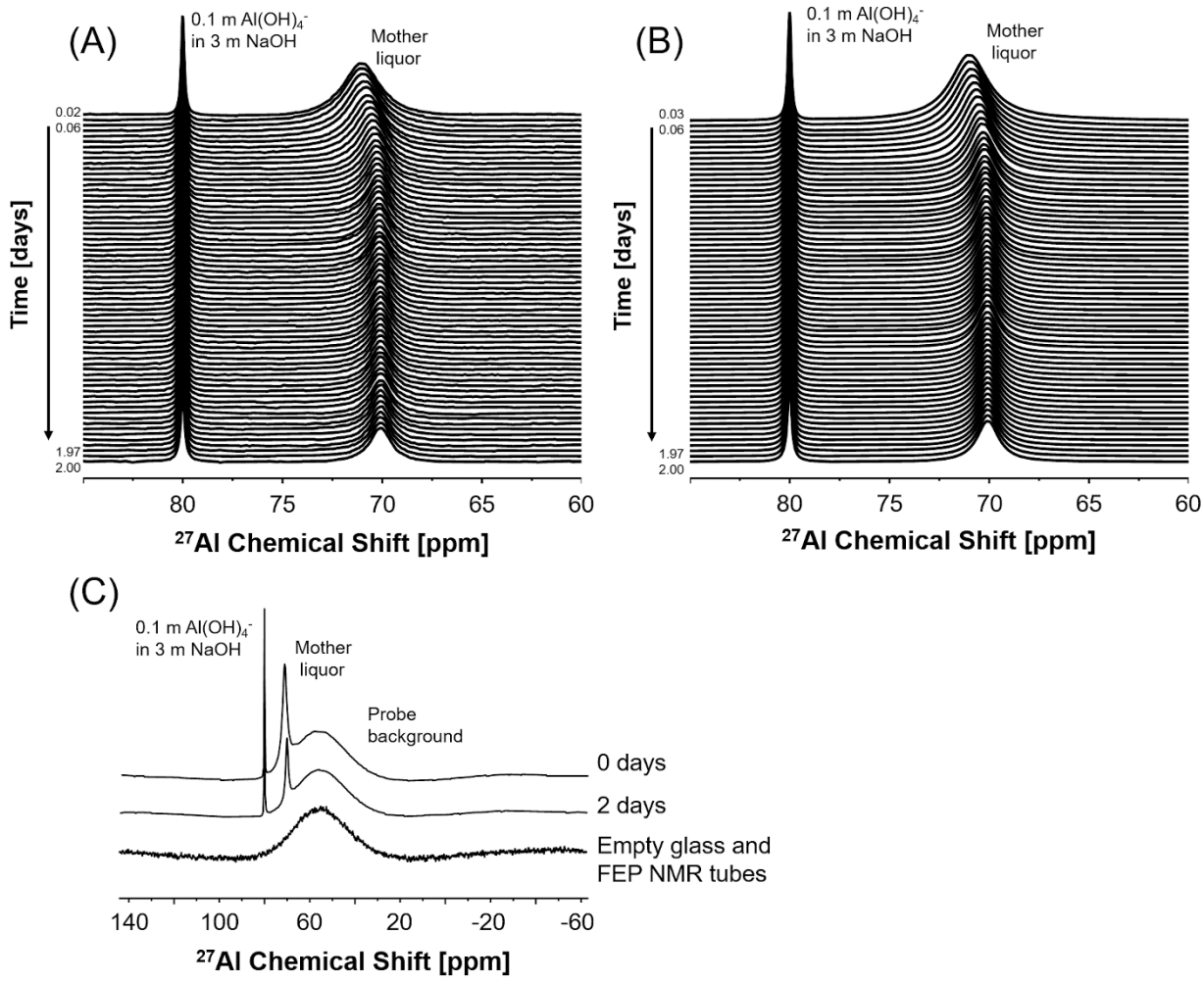

Figure S5. Additional liquid-state ^{27}Al NMR results are shown at 17.6 T and 40°C that were acquired with alternating pulse widths. Spectra acquired with an (A) $\pi/20$ pulse width or a (B) $\pi/2$ pulse width are shown following background correction. The spectra are decimated such that every 4th spectrum is shown for each pulse width. (C) A comparison of the summation of the first five (t=0 days) and last five (t = 2 days) ^{27}Al NMR spectra acquired with a $\pi/20$ pulse without background correction. Acquisition of a ^{27}Al NMR spectra with a $\pi/20$ pulse of an air-filled NMR tube with air-filled, coaxially inserted fluorinated ethylene polypropylene copolymer (FEP) tubes is also shown. The background scan was acquired utilizing an acquisition time of 0.6 s, delay between experiments of 2 s and 20 Hz line broadening, albeit with less transients than the spectra collected at t = 0 and t = 2 days.

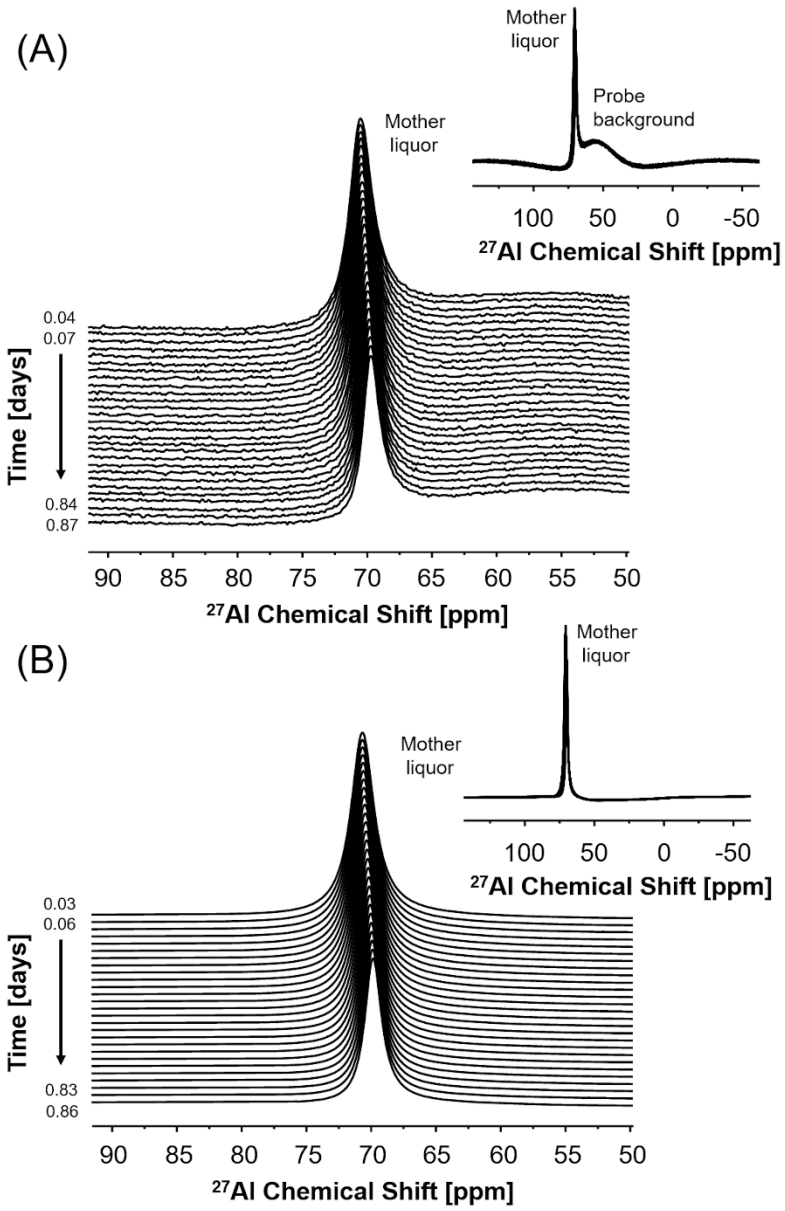

Figure S6. Single pulse, direct excitation liquid-state ^{27}Al NMR results are shown at 17.6 T that were acquired at 40°C with alternating pulse widths, shown without baseline correction. For this experiment, there was no coaxial reference. The spectra acquired with an (A) $\pi/20$ pulse width and a (B) $\pi/2$ pulse width. The acquisition utilized an acquisition time of 0.6 s, 256 transients, a delay between transients of 2 s and 20 Hz line broadening. Every 2nd spectrum is shown for each pulse width. The insets show the same spectra with a greater spectral window and with no offset between spectra to show the lack of additional resonances across a greater chemical shift range and the consistency of the probe background. While the Al^{3+} ions in the mother liquor presents a relatively sharp signal near 70 ppm compared to the probe background at ca. 60 ppm, there is no evidence for additional tetrahedral Al^{3+} resonances near 80 ppm nor octahedral coordinated Al^{3+} resonances near 0 ppm.

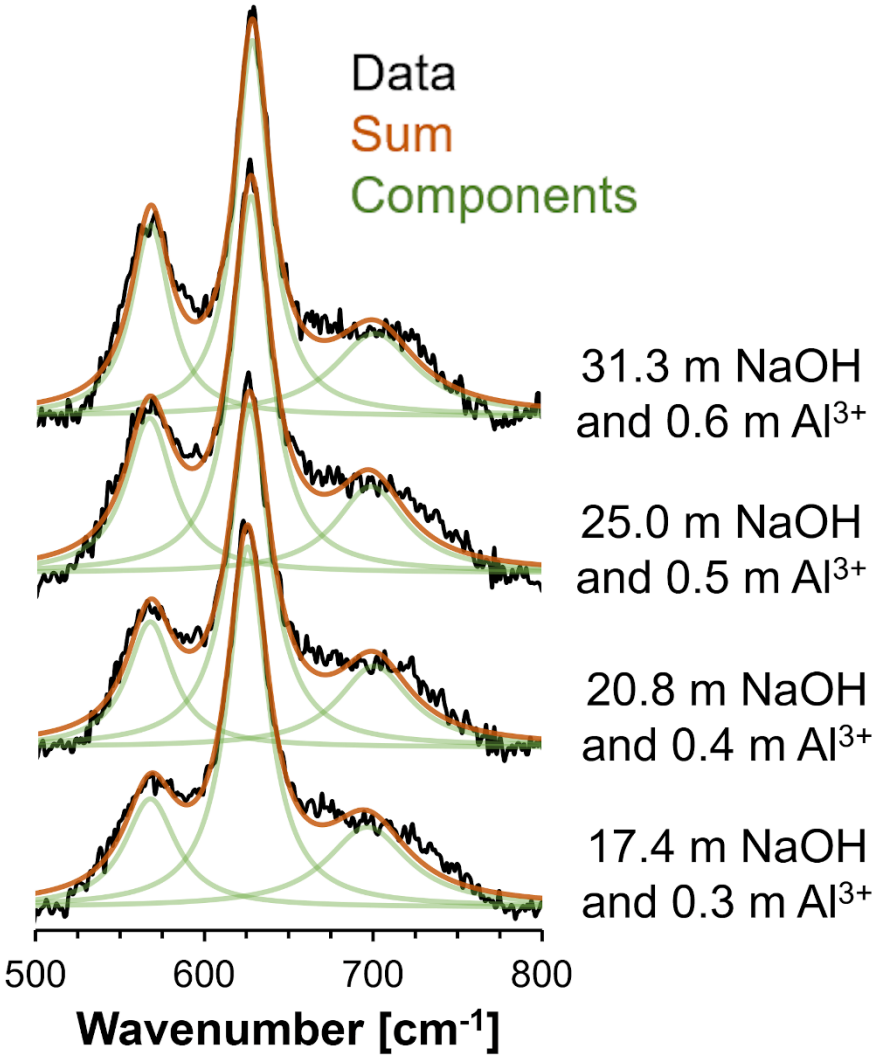

Figure S7. Additional Raman spectroscopy results. The Raman spectrum of the 31.3 m NaOH and 0.6 m Al^{3+} solution is reproduced from the first time point of the series shown in the main text. Additional solutions were prepared to evaluate the side band (568 and 701 cm^{-1}) intensities at more dilute concentrations. The molar ratio of Na^{+} and Al^{3+} remains equivalent between samples, but the amount of water is increased. The spectra are normalized to the same integrated area. The distribution of signal intensity in the side bands at 568 and 701 cm^{-1} in the relatively dilute solutions progressively decreases compared to the 31.3 m NaOH and 0.6 m Al^{3+} solution. The line shape parameters and relative intensities are in Table S3.

Table S2. Line shape parameters for Raman spectra of the mother liquor (Figure 4 in the main text)

Time	Wavenumber [cm^{-1}]	Full width at half maximum [cm^{-1}]	Relative integral [%]
0.0 days	567.7	28.1	27.3
	628.3	25.5	49.3
	701.2	60.3	23.4
0.1 days	567.3	28.4	26.4
	628.0	26.8	48.9
	700.2	59.5	24.7
0.2 days	566.8	26.8	25.7
	627.8	25.9	50.7
	701.0	58.1	23.6
1.0 day	568.9	29.7	24.6
	627.9	30.2	46.1
	697.4	65.9	29.3
2.0 days	568.7	27.4	27.0
	627.9	25.4	50.8
	702.1	52.8	22.2
0.3 m Al^{3+} 3 m NaOH	-	-	-
	623.9	26.1	100
	-	-	-

Table S3. Line shape parameters for Raman spectra of additional solutions (Figure S7)

Composition	Wavenumber [cm^{-1}]	Full width at half maximum [cm^{-1}]	Relative integral [%]
0.6 m Al^{3+} 31.3 m NaOH	567.7	28.1	27.3
	628.3	25.5	49.3
	701.2	60.3	23.4
0.5 m Al^{3+} 25.0 m NaOH	566.8	34.1	25.4
	627.3	28.0	53.1
	698.7	51.0	21.6
0.4 m Al^{3+} 20.8 m NaOH	566.8	33.2	21.9
	626.0	29.7	55.3
	700.5	52.7	22.8
0.3 m Al^{3+} 17.4 m NaOH	568.0	37.3	20.4
	625.6	29.0	55.4
	696.5	58.8	24.1

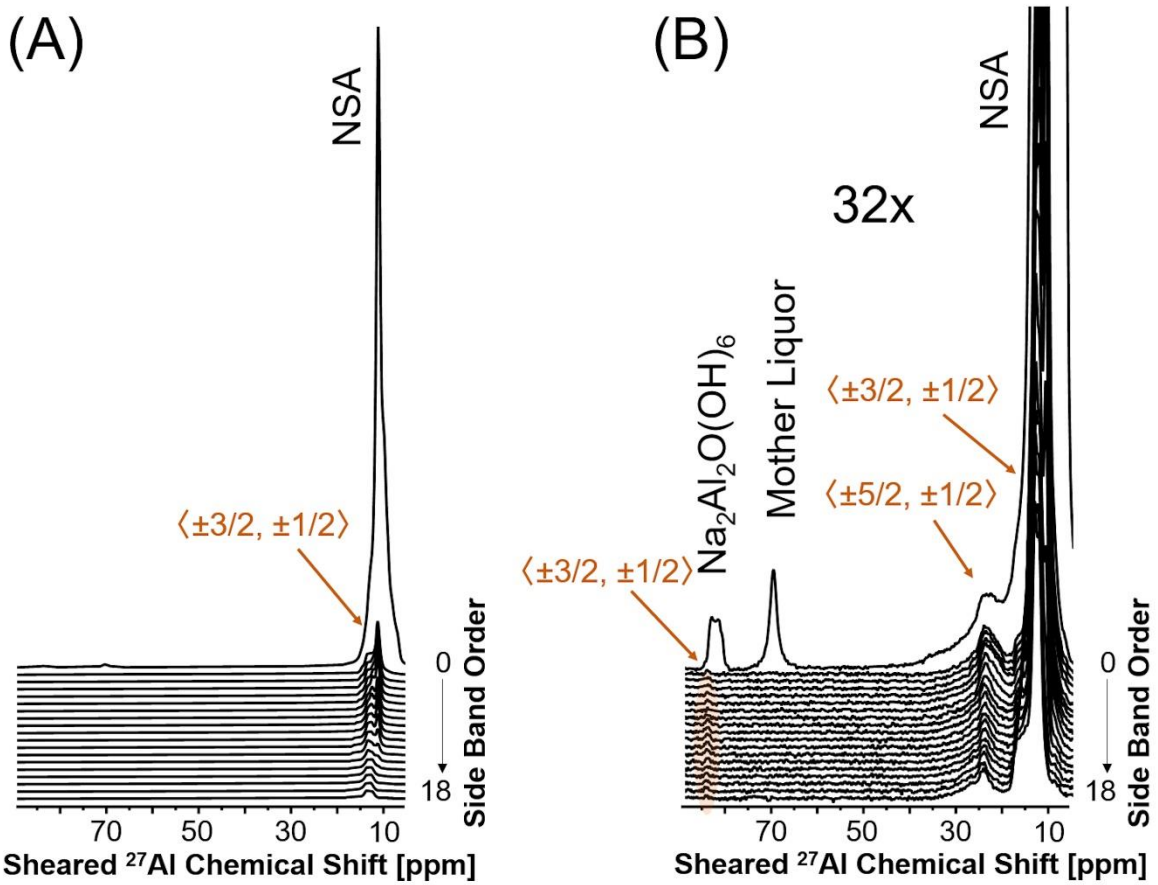

Figure S8. Two-dimensional one pulse $(TOP)^2$ representation of a single pulse ^{27}Al MAS NMR spectrum at 20.0 T of NSA at a magic angle spinning rate of 20 kHz. (A) TOP ^{27}Al MAS NMR spectrum, where the arrow denotes the satellite transitions appearing ca. 11, 15 and 25 ppm. (B) The same spectral window is shown, with 32x vertical magnification. In the TOP MAS NMR method, the 1D MAS NMR spectrum is sheared into regions such that the spinning side bands arising from the central transition are overlaid. This facilitates identification of satellite transitions, which overlap with the central transition, albeit with weak intensity. Notably, the $Na_2Al_2O(OH)_6$ and Mother liquor resonances are not propagated throughout the spinning side band manifold with equal intensity, confirming that they are not satellite transitions of the predominant NSA resonances. Barely present above the noise, is evidence for the satellite transition of $Na_2Al_2O(OH)_6$, which is highlighted orange to guide the eyes. Only spinning sidebands downfield of the central transition are shown, and analysis of upfield spinning side bands leads to analogous results and interpretations of $Na_2Al_2O(OH)_6$ and Mother liquor resonances.

REFERENCES

1. Graham, T. R.; Gorniak, R.; Dembowski, M.; Zhang, X.; Clark, S. B.; Pearce, C. I.; Clark, A. E.; Rosso, K. M. Solid-State Recrystallization Pathways of Sodium Aluminate Hydroxy Hydrates. *Inorg. Chem.* **2020**, DOI: 10.1021/acs.inorgchem.0c00258
2. Massiot, D.; Hiet, J.; Pellerin, N.; Fayon, F.; Deschamps, M.; Steuernagel, S.; Grandinetti, P. J. Two-Dimensional One Pulse MAS of Half-Integer Quadrupolar Nuclei. *J. Magn. Reson.* **2006**, *181*, 310–315, DOI:10.1016/j.jmr.2006.05.007